Journal of Cellular Biochemistry 95:620–631 (2005)

Activation of an Energy Providing Response in Human Keratinocytes After γ Irradiation

Jérôme Lamartine,[1,2] Noreli Franco,[1] Pascale Le Minter,[1] Pascal Soularue,[1] Olivier Alibert,[1] Jean-Jacques Leplat,[3] Xavier Gidrol,[1] Gilles Waksman,[1,2] and Michèle T. Martin[1]*

[1]Service de Génomique Fonctionnelle, CEA, Evry, France
[2]Université d'Evry Val d'Essonne (EA 2541: Université d'Evry/CEA), Evry, France
[3]UMR CEA INRA Radiobiologie et Etude du Génome, Jouy en Josas, France

Abstract We performed a microarray study on human differentiated HaCaT keratinocytes exposed to ionizing radiation (2 or 10 Gy). At 3 h after exposure, more than 150 known and unknown genes were found regulated in irradiated HaCaT keratinocytes. Among the genes regulated at 3 h, those involved in cell energy metabolism appeared to be the most abundant and the most responsive. Two mitochondrial ATP-synthases and several other genes involved in energy producing pathways, such as glucose metabolism, were induced, whereas many genes from energy requiring pathways were shut down. These changes in energy metabolism were confirmed both in normal primary keratinocytes and in HaCaT keratinocytes by RT-PCR and proteins studies. Moreover, measures of intracellular ATP revealed a 50% increase in keratinocytes immediately after irradiation, supporting an energy procurement response. The overall results indicate that irradiation induces an immediate burst of ATP that seems to be a general response of human differentiated keratinocytes to the radiation stress. This article contains Supplementary Material available at http://www.mrw.interscience.wiley.com/suppmat/0730-2312/suppmat/v95.html. J. Cell. Biochem. 95: 620–631, 2005.

Key words: DNA microarrays; γ irradiation; genetic reprogramming; human epidermis; energy metabolism

Skin epidermis is a physiological barrier that protects the organism against pathogens, and chemical or physical damage. Keratinocytes, which are the major cell type in human epidermis, serve as an important sensor between the external environment and the organism, as shown by their innate immune response and interactions with the immune system during wound healing, skin infections, and inflammation. Functional role of keratinocytes can differ according to their differentiation level, which follows a tightly coordinated program. Undifferentiated keratinocytes proliferate in the basal layer, and then progressively differentiate in the upper layers up to the terminal differentiation in the horny layer.

The recent developments in large-scale gene expression analysis, such as microarrays, provide methods for global expression profiling of the response of keratinocytes to environmental changes. These methods have been used to characterize the response of skin keratinocytes to UV irradiation [Li et al., 2001; Sesto et al., 2002; Takao et al., 2002; Dazard et al., 2003]. Thus far, the response of keratinocytes to other environmental hazards has never been studied by microarrays. Ionizing radiation is another physical stress, which targets the keratinocytes specifically, since skin is the first tissue to be irradiated during the external exposures used in radiotherapy. This cancer treatment can induce various deleterious effects in skin, which can appear both during the treatment, such as erythema and desquamation, and several years later, such as carcinoma and late complications. This study describes the first transcriptional profile of human keratinocytes exposed to ionizing radiation. We used the non-tumorigenic HaCaT cell line as a model for human

Grant sponsor: European Union (NAIMORI); Grant number: FIGH-CT-2001-00157; Grant sponsor: Comité de Radioprotection d'Electricité de France.

*Correspondence to: Michèle T. Martin, Service de Génomique Fonctionnelle, CEA, 2 rue Gaston Crémieux, CP5722, 91057 Evry Cedex. France.
E-mail: michele.martin@cea.fr

Received 21 May 2004; Accepted 4 November 2004
DOI 10.1002/jcb.20394

keratinocytes for microarray screening. These HaCaT keratinocytes exhibit large similarities to primary keratinocytes. When grafted into a nude mouse, they are able to reconstitute a whole epidermis [Breitkreutz et al., 1998]. When cultured to confluence, they undergo growth arrest and progressively differentiate, as demonstrated by their stratification and sequential induction of differentiation markers such as keratin K10 and involucrin [Boukamp et al., 1988]. By expression analysis, we have recently shown that most of the markers regulated during the density-induced differentiation of HaCaT cells were also differentiation markers for primary keratinocytes [Lemaitre et al., 2004]. In this work, we used high calcium concentration and high cell density to cultivate HaCaT keratinocytes up to a differentiated state mimicking suprabasal layers of epidermis.

In the present study, we studied the response to γ rays of differentiated HaCaT keratinocytes using microarrays. Differentiated keratinocytes from the suprabasal layers of human epidermis are the first exposed during therapeutical and accidental irradiation. In cases of localized accidental exposures, they could be used to estimate the doses received by patients since they can easily be obtained by epidermis stripping, from some hours to several days following the accident. It is, therefore, important to identify biological markers of radiation exposure in these differentiated skin cells.

We found that the molecular response of differentiated HaCaT keratinocytes was characterized by a global and transient reprogramming at 3 h, with striking regulations of genes involved in energy production. Measures of intracellular ATP performed both in HaCaT and normal keratinocytes revealed an immediate burst of ATP that seems to be a general response of human differentiated keratinocytes to the radiation stress.

MATERIALS AND METHODS

Cell Culture and Irradiation

HaCaT keratinocytes were seeded at 10,000 cells/cm^2 and cultured as monolayers in DMEM at high calcium concentration (1.8 mM) supplemented with 10% fetal calf serum, at 37°C and 5% CO_2. At day 7, the culture was confluent, and cells were further incubated for another 3 days to reach a differentiated state. Cell cycle analysis was performed as described [Tani et al., 2000] in two independent experiments on a MoFlo analyzer (Cytomation). Flasks were irradiated with a ^{60}Co source at a dose rate of 0.4 Gy/min. Two doses of ionizing radiation were used: the 2 Gy standard dose of radiotherapy fraction and a high dose of 15 Gy.

Human normal keratinocytes were isolated with trypsin from mammary skin biopsies obtained from plastic surgery (AFM-BTR, La Pitié-Salpétrière, Paris) and primary cultures were initiated in KGM2 (Clonetics) on flasks coated with collagen type I (Falcon Biocoat). The differentiation program of secondary cultures was induced at confluency by a switch to the following differentiation medium: KBM (Clonetics) supplemented with 0.5 μg/ml hydrocortisone, 5 μg/ml insulin, 5 ng/ml EGF, and 1.8 mM calcium for 3 days. To study in vivo the early response of human skin, a surgical biopsy of normal mammary skin was cut into several pieces and incubated in Petri dishes in cell culture medium. Half of the dishes were exposed to 2 Gy with the cobalt source, and then returned to incubator. Samples were collected at 24 h after irradiation and processed for immuno-histochemical studies.

Microarray Production

Two types of DNA collections for preparing the cDNA arrays: (a) a collection of 5,760 cDNA clones from the human infant brain 1NIB library kindly provided by Genethon [Soares et al., 1994]; (b) a collection of more than 2,300 human genes corresponding to specific keywords (apoptosis, differentiation, adhesion, DNA repair...) selected by direct interrogation of the Unigene database. Primers were designed to amplify a 400–600 bp product for each ORF using a mixture of cDNAs obtained from various cell lines as templates. The uniqueness of the PCR primers and the absence of cross matching for each PCR product were checked using an automatic blast interrogation.

The PCR products were prepared in 96-well plates, purified by ethanol precipitation, washed in 70% ethanol, dried, dissolved in TE/DMSO (50/50), and stored at −80°C. PCR products were arrayed on amino-silane coated glass slides (Corning CMT-GAPS II) using a MicroGrid-II Micro-arrayer (BioRobotics). These home-made microarrays have already been used in a study on human keratinocytes [Lemaitre et al., 2004].

A complete description of the microarrays used in this study including the protocols for production and post-processing of slides has been deposited into the GEO database (www.ncbi.nlm.nih.gov/geo/). This information is available under the following GEO accession numbers GPL258, GPL259, GPL261.

RNA Isolation, cDNA Synthesis, and Labeling

Total RNA was isolated using the Tripure reagent (Roche Molecular Biochemicals) following the manufacturer's instructions and dissolved in RNAse-free water. The quality of RNA was controlled using an Agilent 2100 Bioanalyzer (Agilent Technologies) and concentration was measured by absorbance at 260 nm. Labeling of total RNA was performed by coupling with aminoallyl-modified dUTP (Sigma), followed by a subsequent incorporation of monofunctionnal Cy3 or Cy5-N-succinimide esters (Amersham Biosciences). For each labeling experiment, 20 μg of total RNA was used in an oligo(dT) primed reaction. The protocols for labeling, hybridization and washing are available in the GEO database under the accession number GSM4651.

Microarray Data Analysis

Fluorescence intensities of Cy3 and Cy5 were measured separately at 532 and 635 nm with a laser scanner (Axon Genepix4000A). The resulting 16-bit data files were imported into an image analysis Program (Genepix 2.0, Axon Instruments). Feature ratios were calculated after background subtraction using GenePix 2.0 software, which flags spots as absent based on spot characteristics. Additionally, bad spots were manually flagged. These flagged spots (less than 1%) were not included in subsequent analyses. Data were normalized using a global and linear normalization method: they were scaled such that the average median ratio values for all spots were normalized to 1.0. Additionally, only spots that had more than 70% of their pixels greater than 2 standard deviations above the background in one of the two wavelengths were selected for further analysis. The data files for all our hybridizations are available in the GEO database under the accession number GSE337.

To determine the proportion of false positives, we performed 4 hybridizations using a human control RNA representing 10 different human cell lines (Stratagene Universal human reference RNA) labeled with Cy3 and Cy5. Using the normalization and analysis methods described previously to search for genes, which were differentially expressed, we found no gene showing more than a 1.4-fold change. We therefore considered that under our experimental conditions, a 1.5-fold ratio was significant to discriminate between technical background and biological regulation.

RT-PCR

Total RNA was diluted in DEPC-treated water to 0.2 μg/μl, denatured at 70°C for 10 min, and quickly chilled on ice. Ten microliters of the total RNA was mixed with 500 ng oligo(dT)12–18 (Invitrogen), 12 μl of RT-mix (50 mM Tris-HCl, pH 8.3, 75 mM KCl, 3 mM $MgCl_2$, 10 mM DTT), 0.5 mM dNTPs, and 200 units Superscript II (Invitrogen) and incubated for 1 h at 42°C. After cDNA synthesis, the reaction mixture was incubated for 10 min at 70°C and then diluted with H_2O into a final volume of 50 μl. All PCR reactions were conducted with 3 μl of diluted cDNA using the primers designed for the amplification of the human ORFs used for microarray spotting (see above Microarray Production). In order to assess the linearity of the amplification, a dilution series of HaCaT RNA was generated for use as standards in RT-PCR. The number of cycles was chosen for each primer pair to ensure linearity of amplification on this standard series. The annealing temperature was 58°C for all genes.

PCR products were resolved in 2% agarose gels and visualized by ethidium bromide staining on a digital video system. Densitometric analysis of gel images was performed using BioProfil Bio1D software (Vilbert Lourmat Technology): the total intensity of each band was measured as the integrated volume of pixels associated with each ethidium bromide-stained band. PCR experiments were performed two times for each time point.

Western Blotting

For preparation of whole cell lysates, cells were washed twice with PBS and lysed for 20 min on ice in lysis buffer containing 20 mM Tris-HCl pH 8.0, 150 mM NaCl, 1% NP-40, 5% glycerol and a cocktail of protease inhibitors (Complete tablets, Roche). The lysates were centrifuged at 12,000*g* for 35 min at 4°C. The protein concentrations were determined with

the Bio-Rad Protein assay reagent. Proteins (30 μg) were loaded on NuPage Novex® 4–12% pre-cast gel (Invitrogen), transferred to a PVDF membrane and blocked in 5% BSA or 10% non-fat milk in TBS-T (Tris buffer saline-Tween). The membrane was incubated overnight at 4°C in TBS-Tween with primary antibody specific for cytochrome-*c* (1:1,000 dilution, Novabiochem), ATP1a1 (1:5,000 dilution, AbCam), or beta-tubulin (1:1,000 dilution, Zymed) as control and then washed with TBS-T, incubated with a 1:10,000 dilution of anti-rabbit or 1:2,000 dilution of anti-mouse HRP-conjugated secondary antibodies 45 min at room temperature, and visualized with the ECL detection kit (Amersham Biosciences). Densitometric analysis of gel images was performed using BioProfil Bio1D software (Vilbert Lourmat Technology).

Immunohistochemistry

Normal skin was obtained from breast skin biopsies from the Tissue Bank for Research (AFM-BTR, La Pitié-Salpétrière, Paris). Samples of normal and irradiated skin (2 and 15 Gy) were fixed in 10% formalin-buffered solution and embedded in paraffin wax. Serial 5-μm sections were cut, dewaxed, and treated for immunohistochemical detection. To unmask antigen, a chemical and heat treatment was performed by incubating sections in a 10-mM sodium citrate buffer, pH 6 at 95°C for 10 min. For permeation, sections were incubated in a 0.1% Triton X100-PBS solution. Then, sections were incubated for 10 min in a 3% H_2O_2 solution prepared just before use to quench endogenous peroxidases and in a 10% sheep serum PBS or in a 3% BSA/PBS solution for 1 h to block non-specific sites. Sections were incubated overnight at 4°C in a PBS solution containing specific primary antibodies at a dilution of 1:1,000 for ATP1a1, and 1:10 for cytochrom c. These antibodies were revealed by the LSAB®2 kit (DAKO). Slides were submitted to sequential 10 min incubations with biotin-linked anti-mouse or anti-rabbit antibody and peroxidase-labeled streptavidin followed by a diaminobenzidine treatment (DAB+, DAKO) and a final counterstaining using hematoxylin.

ATP Measurement

Intracellular ATP was measured by bioluminescence using the ViaLight HS kit (BioWhittaker). Keratinocytes were cultured in 96-well plates (Becton Dickinson) and differentiated under high cell density and high calcium concentration as described in cell culture methods. Three, 6 or 24 h after irradiation with 2 or 15 Gy, 100 μl of lysis buffer was added to 100 ul of culture medium, and 180 μl of the mixture was put into white-walled 96-well plates. Irradiated and non-irradiated cells were then processed using the manufacturer's protocol and light emission was quantified using a Micro-Lumat LB96 luminometer (EGG Berthold). In each plate, eight measurements per dose and per unit of time were carried out. Three independent cell cultures were processed for both the HaCaT cell line and primary keratinocytes.

RESULTS AND DISCUSSION

Cellular Model

Each layer of the epidermis can react differently to environmental stress according to keratinocyte differentiation. In this work, we addressed the response of differentiated keratinocytes to γ irradiation using microarrays. HaCaT keratinocytes were differentiated in culture by high density and calcium. The cell cycle status of the control cultures was studied by flow cytometric analysis after propidium iodide staining: 90% of the cells cultured for up to 10 days were found to be in the G0/G1 phase of the cell cycle (data not shown). The differentiation state of the cells was evaluated by expression analysis of several differentiation

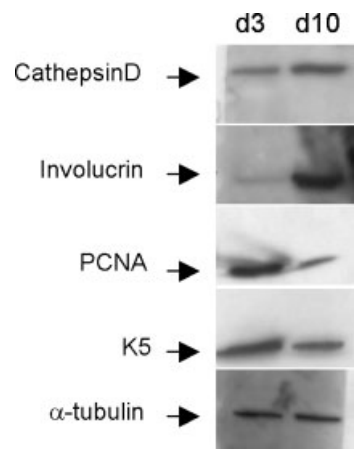

Fig. 1. Expression analysis of proliferation and differentiation markers in cultured HaCaT cells. Total proteins (25 μg) extracted from HaCaT cells cultured for 3 days (d3) or 10 days (d10) were loaded on SDS–PAGE, electro-transferred on a nylon membrane, and proteins were specifically revealed using antibodies. Alpha tubulin was shown as a representative loading control.

and proliferation markers (Fig. 1). Strong downregulation of PCNA confirmed the cell cycle arrest. An increased expression of involucrin and cathepsin D, together with a reduced expression of keratin 5, revealed an advanced state of differentiation after 10 days of culture. Then we studied whether immediate toxicity was induced in HaCaT keratinocytes by radiation exposure. For that purpose, cytotoxicity in irradiated cells (2 and 15 Gy) was compared to that of mock-irradiated cells. At 3 and 8 h after the treatment, immediate viability was not affected by irradiation, as an average 5% mortality was observed in both treated and control cultures by Trypan-blue staining (data not shown).

Global Expression Changes in γ-Irradiated HaCaT Keratinocytes

cDNA microarrays containing more than 8,000 probes were used to quantitatively assess changes in gene expression after γ irradiation. Samples were collected at 3 and 24 h after irradiation, during the immediate cellular response, and microarray hybridizations were carried out using dye-swap. To ensure the reliability of data, samples from each dose and time point were reciprocally labeled in four hybridization experiments (two dye-swaps). The genes that showed differential expression after irradiation were selected based on a 1.5-fold change in the ratio for the four hybridizations (see Materials and Methods). Data from reciprocal replicates were averaged after independent global and linear normalization. Attention was paid to genes represented by multiple probes on the array, such as VDCA2 or HDLBP (Table I) as well as ITGA6, BTF3, SPARC, PCNA, or MYC (see supplemental data). Although the values of the expression ratio varied, we found similar patterns of regulation for these multiple probes, demonstrating the

TABLE I. Metabolism Genes Up- or Downregulated at 3 h by Ionizing Radiation in HaCaT Keratinocytes

Genbank no.	Symbol	Gene description	Fold induction ± SD	
			2 Gy, 3 h	15 Gy, 3 h
U51478	ATP1B3	ATPase Na+/K+ s.u 3	3.03 ± 0.65	3.13 ± 0.48
F05182	ATP1A1	ATPase Na+/K+ s.u 1	1.86 ± 0.01	2.16 ± 0.06
U05598	AKR1C2	Aldo-keto reductase family 1	2.91 ± 0.65	2.85 ± 1.27
Z14244	COX7B	Cytochrome-*c* oxidase 7B	2.45 ± 0.73	2.71 ± 0.11
X13923	COX6B	Cytochrome-*c* oxidase 6B	2.58 ± 1.28	2.5 ± 0.90
Z42038	SLC1A2	Solute carrier family 1 A2	2.26 ± 0.31	2.37 ± 0.20
F05550	HADHA	HydroxyacylCoA dehydrogenase	2.28 ± 0.13	1.96 ± 0.38
F05194	UQCRC2	Ubiquinol Cyt C reductase	2.02 ± 0.08	2.29 ± 0.13
U09813	ATP5G3	ATPase H+ mitochondrial	2.16 ± 1.23	2.07 ± 0.58
F05518	ATP5C1	ATPase H+ mitochondrial	2.1 ± 0.06	1.93 ± 0.12
F05834	ATP6E	ATPase H+ lysosomal	2.02 ± 0.08	2.01 ± 0.09
F05266	LDHA	Lactate dehydrogenase	2.13 ± 0.20	1.73 ± 0.13
M75161	PFKP	Phosphofructokinase	1.95 ± 0.45	2.22 ± 0.65
Z42672	OXA1L	Cytochrome-*c* oxidase	2.02 ± 0.25	1.97 ± 0.22
J03037	CA2	Carbonic anhydrase II	2.02 ± 0.4	1.91 ± 0.34
F06593	VDAC2	Voltage-dependent anion channel 2	2.1 ± 0.35	1.9 ± 0.24
L06328	VDAC2	Voltage-dependent anion channel 2	1.75 ± 0.08	1.65 ± 0.06
X00737	NP	Nucleoside phosphorylase	1.68 ± 0.05	2.19 ± 0.24
J04058	ETFA	Electron transfer flavoprotein	1.78 ± 0.5	2.04 ± 0.13
U59309	FH	Fumarate hydratase	1.64 ± 0.04	2.0 ± 0.09
F06300	AKR1C3	Aldo-keto reductase family 1	1.72 ± 0.17	1.87 ± 0.11
J04173	PGAM1	Phosphoglycerate mutase	1.81 ± 0.91	1.54 ± 0.48
V00572	PGK1	Phosphoglycerate kinase	1.2 ± 0.12	1.52 ± 0.23
F05706	HCS	Cytochrome-*c*	1.6 ± 0.05	1.82 ± 0.13
M27396	ASNS	Asparagine synthase	−4.16 ± 0.7	−4.46 ± 0.53
F06628	HDLBP	High-density lipoprotein binding prot.	−2.43 ± 0.06	−2.22 ± 0.12
F05347	HDLBP	High-density lipoprotein binding prot.	−2.4 ± 0.14	−1.8 ± 0.08
M90516	GFPT1	Glucose 6P transaminase	−1.78 ± 0.31	−1.72 ± 0.20
X01630	ASS	Argino succinate synthase	−1.36 ± 0.55	−2.0 ± 0.37
M77693	SAT	Spermine acetyl transferase	−1.5 ± 0.46	−1.52 ± 0.17
D87328	HLCS	Holocarboxylase synthase	−1.69 ± 0.10	−1.81 ± 0.12
U47025	PYGB	Glycogen phosphorylase	−1.54 ± 0.06	−2.12 ± 0.23
M61831	AHCY	S-adenosyl homocysteine hydrolase	−1.23 ± 0.16	−1.6 ± 0.22

The first column lists the accession number of the entries. The second and third columns contain the symbol and description of each induced gene functionally classified. The fold induction or repression at the indicated point is given as the mean ratio of four chips, the corresponding standard deviation is indicated.

TABLE II. Percentage of Analyzed DNA Spots Regulated by Ionizing Radiation in HaCaT Keratinocytes

	3 h			24 h		
Dose	Induced (%)	Repressed (%)	Total (%)	Induced (%)	Repressed (%)	Total (%)
2 Gy	2	1.9	3.9	0.26	0.2	0.46
15 Gy	3.8	3	6.8	0.7	1.2	1.9

Total number of analyzed spots: 3,500; the given percentage is the mean of four hybridizations per point (two dye swaps) with a fold ratio higher than 1.5 in the four hybridizations. To estimate the false positive rate, control hybridizations were performed using the same RNA (HaCaT, 0 Gy, 3 h) labeled with Cy3 and Cy5. Under these conditions, we found no gene with a ratio higher than 1.4 for induced genes or lower than 0.7 for repressed genes.

reliability of the probes and the robustness of the method.

The percentage of differentially regulated genes was found higher after 15 Gy than 2 Gy (Table II). However, the effect of the dose was not striking, as most of the genes induced or repressed at 2 Gy were also responsive to 15 Gy. A striking aspect of the data is the difference between the number of genes regulated at 3 and 24 h after irradiation. Only a small fraction of genes was modulated at 24 h, and most of these genes were different from those regulated at 3 h. As the immediate gene response was strong at 3 h but seemed to be lost at 24 h, we focused our attention on the genes regulated at 3 h after irradiation, corresponding to the first wave of the genetic reprogramming. Only DNA spots corresponding to genes with a known protein function (about 65% of analyzed spots) were further investigated.

RT-PCR was performed to confirm microarray results. The expression of 25 genes, which were up- or downregulated by irradiation from several functional groups, was verified by RT-PCR. For each gene, PCR conditions were adjusted to ensure linearity of the amplification. Some examples of RT-PCR results are shown in Figure 3. RT-PCR confirmed the microarray results for 22 of these 25 genes. For three genes, we were unable to detect either induction or repression by RT-PCR.

To help elucidate the molecular responses that take place in irradiated keratinocytes, the transcripts were classified according to their biological functions on the basis of the Gene Ontology Consortium (GO, biological process categories) [Ashburner et al., 2000]. We classified therefore 157 known genes representing 92 upregulated and 65 downregulated genes at 3 h (Fig. 2). Many genes already published as induced by ionizing radiation, including ACTB [Woloschak et al., 1990] encoding beta-actin, CAT [Hardmeier et al., 1997] encoding catalase, COX6B and COX7B [Balcer-Kubiczek et al., 1998] encoding cytochrome-*c* oxidase, or HSP27 [Fornace et al., 1989] encoding a heat shock protein, were found to be upregulated in our study (see Table I and supplemental data), thus validating our experimental design.

Changes in DNA Repair and DNA Metabolism Gene

Radiation produces a large spectrum of lesions, including DNA single and double-strand breaks, deletions, or rearrangements. Mammalian cells possess several efficient systems for repair of those lesions in DNA. In the present study, we found no induction of genes directly involved in DNA repair activity in irradiated keratinocytes. This is in accordance with other studies, and can be explained by the fact that the major regulations of most proteins involved in DNA repair do not occur at the transcriptional level. For example, using microarrays with the totality of the yeast coding

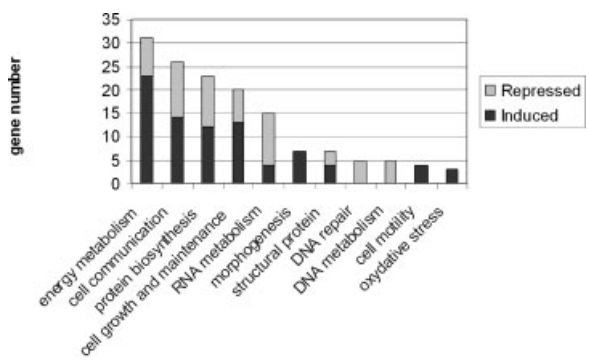

Fig. 2. Functional classification of genes regulated by irradiation in HaCaT cells. The 157 known genes were classified according to their biological functions on the basis of the Gene Ontology Consortium (GO, biological process categories). The number of genes in each functional categories is given (black: induced; gray: repressed).

sequences, Birrell et al. [2002] found no induction of DNA repair genes after exposure to DNA-damaging agents, including γ rays. Surprisingly, we found that five DNA repair genes, notably three genes from the MSH family (MSH2, MSH3 and MSH6), were downregulated 3 h after irradiation (see Table III in Supplementary Material at http://www.mrw.interscience.wiley.com/suppmat/0730-2312/suppmat/v95.html). We also confirmed the downregulation of MSH2 at the protein level by Western blotting (data not shown). Such inhibition has not yet been described after treatment with other DNA damaging agents. MSH proteins are essentially involved in the repair of base-mismatch, a defect rarely caused by γ rays. The observed downregulation of the MSH transcripts could reflect a complex regulation of the DNA repair activity after γ irradiation or be linked to other activities of MSH proteins. Moreover, it should be noted that in the present study, three genes involved in the initiation of DNA replication (PCNA, MCM7, and PRIM1) were also downregulated (see Table III in supplemental data). These downregulations probably reflect an inhibition of replication as already described by others in response to DNA damage [Stokes and Michael, 2004].

Changes in Cell Energy Metabolism

Many of the genes immediately induced after exposure were involved in energy metabolism. We identified 31 genes involved in cell energy metabolism representing more than 20% of the radiation responsive genes (Fig. 2; Table I). For example, two ATP-dependent pumps were upregulated: the Na^+/K^+ exchange complex (ATP1B3, ATP1A1) and the lysosomal H^+ pump (ATP6E). A striking result was the regulation of many genes directly or indirectly involved in energy production. Thus two genes encoding sub-units of the mitochondrial ATP synthase (ATP5G3, ATP5C1) were strongly induced, as well as several genes coding for proteins of the mitochondrial respiratory chain (cytochrome-*c*, cytochrome-*c* oxidase 6B and 7B, cytochrome oxidase assembly 1-like), for mitochondrial proteins involved in ionic transfer (voltage-dependent anion channel 2), and oxidative phosphorylation (ubiquinol cytochrome-*c* reductase) (Table I). Other induced genes were involved in glycolysis (phosphoglycerate mutase, phosphoglycerate kinase-1, triose phosphate isomerase), glucose metabolism (PFKP) and transport (SLC1A2). Finally, several genes coding for proteins involved in mitochondrial fatty acid catabolism were induced by radiation (aldo-keto reductase, hydroxyacyl coA dehydrogenase and electron transfer flavoprotein). On the other hand, many genes coding for energy-requiring pathways were shut down. For example, several enzymes involved in the biosynthesis of amino acids (asparagine synthase, s-adenosyl homocysteine hydrolase, and glucuronidase beta), in the synthesis of amino-acid-tRNA (isoleucine t-RNA synthase, alanyl-tRNA synthase, glycyl-tRNA synthase, threonyl-tRNA synthase, and cysteinyl-tRNA synthase) or in beta-oxydation of lipids (high density lipoprotein, argino-succinate synthase, holocarboxylate synthase) were repressed in response to γ rays. From these microarray data, we postulated that irradiation induced an immediate energy production in HaCaT keratinocytes that could be linked to ATP synthesis.

The results obtained by microarrays were confirmed with various techniques. The induction of four ATPases in HaCaT cells at 3 h after irradiation was confirmed by RT-PCR (Fig. 3). To analyze the consequences of these mRNA changes at the protein level, we performed Western blotting when antibodies were available. For cytochrome-*c* and ATPase 1A1, the protein expression was induced at 3 h in HaCaT keratinocytes (Fig. 4). By RT-PCR, we analyzed some of the markers found regulated in HaCaT cells in normal primary keratinocytes. Normal keratinocytes were cultured for 10 days up to a differentiated non-proliferative state similar to that obtained in HaCaT cells. We globally confirmed the regulation of genes encoding proteins involved in ATP metabolism (Fig. 5): the mitochondrial H^+ transporting ATP synthase (ATP5C1 and ATP5G3 sub-units) was induced, as well as the lysosomal H^+ ATPase (ATP6E). A gene encoding a protein from the mitochondrial respiratory chain (cytochrome-*c*) was also upregulated. The expression of cytochrome-*c* and ATP1A1 was further investigated in samples of normal mammary skin. These samples were maintained in culture medium, irradiated, and then prepared for immuno-histochemistry at 3 and 24 h after exposure. We observed an expression of ATP1a1 in the more differentiated layer of irradiated epidermis at 24 h after irradiation, whereas no specific expression was detectable in control skin (Fig. 6). As the time point of induction differed from that obtained in cultured HaCaT keratinocytes, we

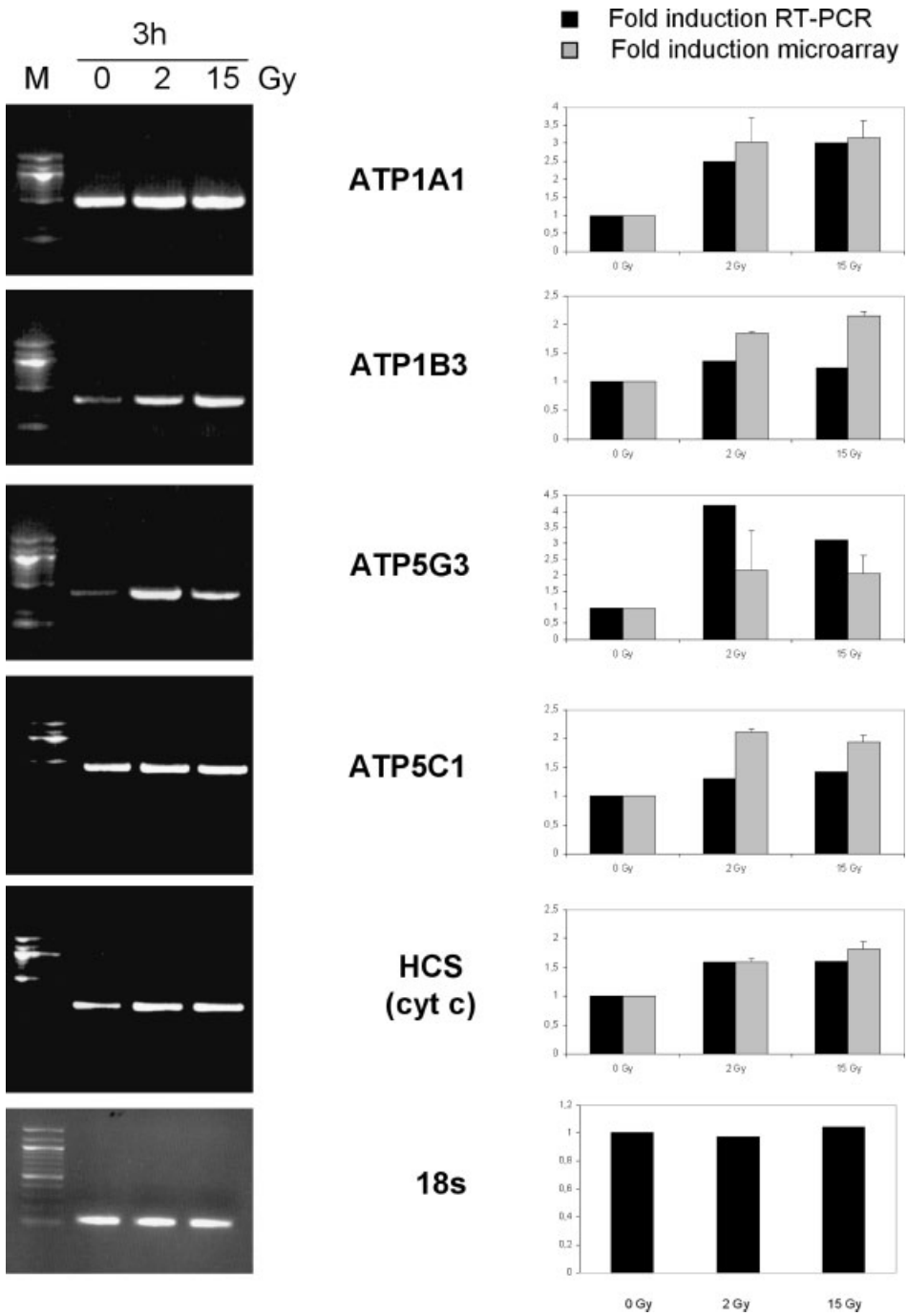

Fig. 3. Expression of genes involved in cell energy metabolism and ionic transport in HaCaT cells. RNA was prepared from HaCaT keratinocytes at 3 h after exposure to 2 or 15 Gy and subjected to RT-PCR reaction using primers pairs for ATP1A1, ATP1B3, ATP5G3, ATP5C1, HCS, and 18S as control. The number of PCR cycles employed for each gene was selected to ensure the linearity of amplification: 30 cycles for ATP1B3, ATP5G3, and ATP5C1; 32 cycles for ATP1A1; 35 cycles for HCS; and 22 cycles for 18S. M: Molecular weight (100-bp DNA ladder). **Left**: Representative PCR gels of RT-PCR products; **Right:** densitometric analysis of RT-PCR products and corresponding microarray results. RT-PCR product yield is expressed in terms of the integrated volume of pixels associated with each ethidium bromide-stained band. The ratio of the intensity of bands corresponding to irradiated/non-irradiated cells is given (black boxes). The corresponding microarray ratio is indicated: mean ± SEM (gray boxes).

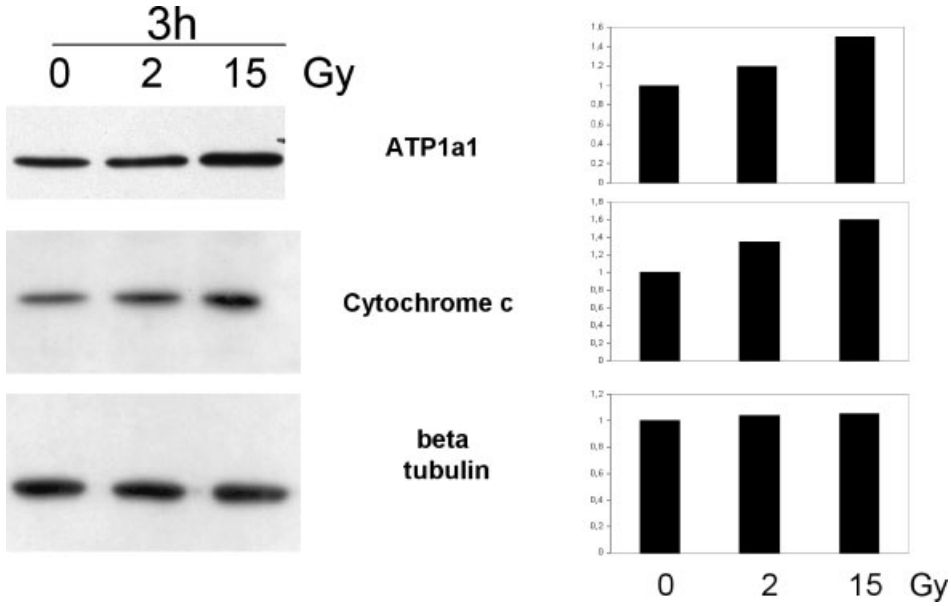

Fig. 4. Western blot analysis of proteins involved in cell energy metabolism and ionic transport. Protein extracts prepared from irradiated HaCaT keratinocytes were harvested at 3 h after irradiation. Beta-tubulin was used as a loading control in a parallel gel. **Left**: Western blot image; **Right:** densitometric analysis of proteins bands. The ratio of the intensity of bands corresponding to irradiated/non-irradiated cells is given.

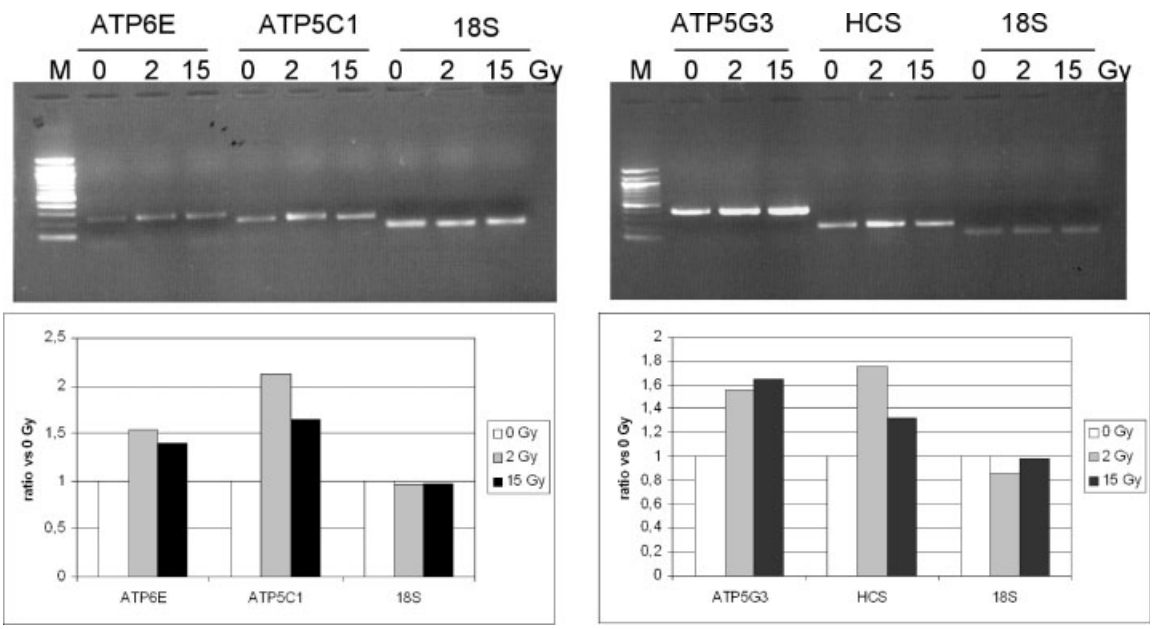

Fig. 5. RT-PCR analysis of metabolism genes in primary keratinocytes. RNAs were prepared from primary normal keratinocytes treated with the indicated doses, harvested 3 h after exposure and subjected to RT-PCR reaction as indicated under Materials and Methods. The number of PCR cycles employed for each gene was selected to ensure the linearity of amplification: 30 cycles for ATP5G3, ATP6E, and ATP5C1; 35 cycles for HCS; and 22 cycles for 18S. M: Molecular weight (100-bp DNA ladder). **Top**: Representative PCR gels of RT-PCR products; **Bottom:** densitometric analysis of RT-PCR products. RT-PCR product yield is expressed in terms of the integrated volume of pixels associated with each ethidium bromide-stained band. The ratio of the intensity of bands corresponding to irradiated/non-irradiated cells is given.

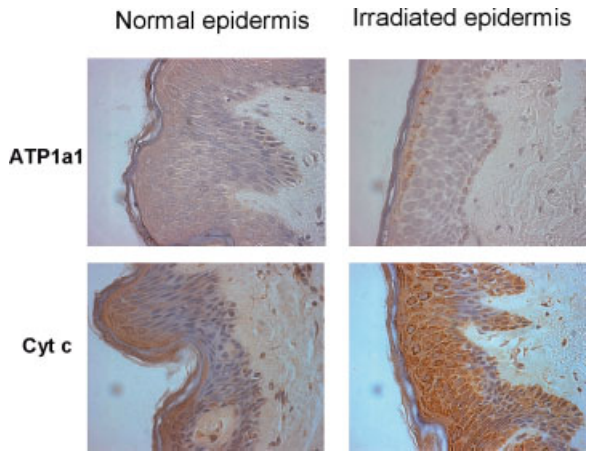

Fig. 6. Expression in irradiated skin. Two proteins involved in cell energy metabolism (ATP1a1 and cytochrome-*c*) found induced in HaCaT keratinocytes after irradiation were analyzed by immunohistochemistry in normal and irradiated mammary skin prepared at 24 h after irradiation at 2 Gy. Original magnification: 63 ×.

speculated that this difference could be explained either by a specific response of HaCaT compared with normal keratinocytes or by the different microenvironments found in vivo and in vitro. For cytochrome-*c*, a strong induction of the protein was observed in irradiated skin, with a modification of the protein localization: the expression was detectable only in the granular layer of the control epidermis, whereas cells from the spinous and granular layers expressed the protein after irradiation (Fig. 6). This result was obtained at both 3 and 24 h after irradiation.

Finally, a functional test was also performed by measuring intracellular ATP levels in control and irradiated cells. We first applied this test to differentiated HaCaT keratinocytes (Fig. 7). We measured a significant increase of ATP in these cells at 3 h after exposure (1.6-fold induction in irradiated cells). This irradiation-dependent increase was almost lost at 6 h after irradiation, and at 24 h the ATP level was lower than in non-irradiated cells. These results confirmed the hypothesis suggested from the microarray data: production of ATP in irradiated HaCaT keratinocytes occurs immediately after irradiation. In order to verify whether the process of ATP production observed in HaCaT cells also occurred in normal cells, we performed the same analysis in primary normal human keratinocytes cultured up to a differentiated state. The ATP burst was observed in these cells as well (1.6–1.8-fold induction), occurring at 6 h after irradiation at 2 and 15 Gy. This early induction was followed by reduced ATP levels at 24 h after irradiation. The observation of an ATP increase in HaCaT cells as well as in primary keratinocytes suggests that this metabolic response can be generalized to all differentiated keratinocytes.

In the present study, we used the microarray technique to screen for new genes and pathways involved in cell response to gamma irradiation. We decided to make this screen on the human HaCaT keratinocyte cell line, which is the only reference for non-cancer keratinocyte cell line. HaCaT keratinocytes exhibit a classical sensitivity to radiation (Do = 1.27 Gy) [Mendonca

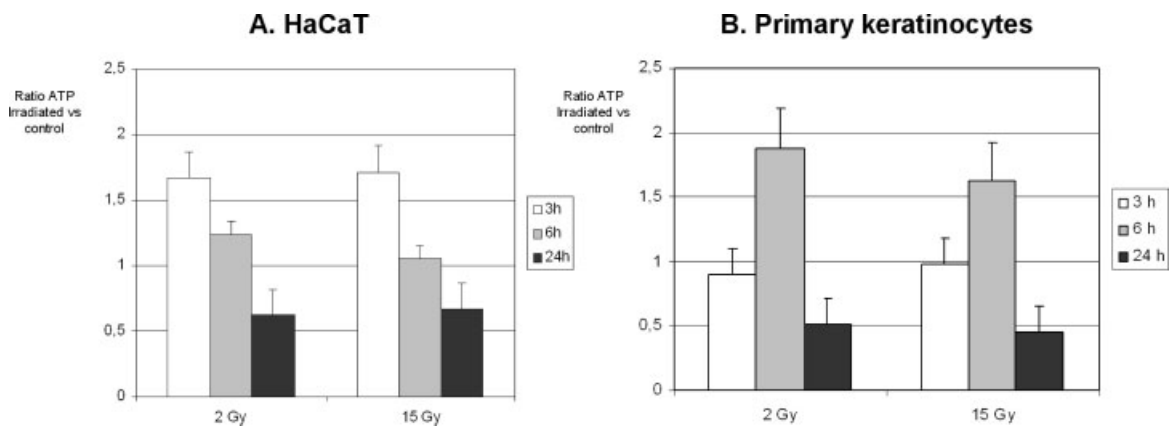

Fig. 7. Variations of ATP levels in irradiated keratinocytes. Intracellular ATP was measured in control and irradiated keratinocytes using the Vialight HS kit (BioWhittaker). Eight measurements were performed per dose and per time. This measurement is based on the luciferase activity, which catalyzes the formation of light from ATP and luciferin. The emitted light intensity was measured using a luminometer. The ratio of the mean value ± SD of the ATP concentration in irradiated cells to non-irradiated cells is given at different times after irradiation.

et al., 1991]. It is widely used in the field of stress research, including UV [He et al., 2004], ionizing radiation [Seymour et al., 2003], and oxidative stress [Huang et al., 2004]. They have also been frequently used in studies on cell apoptosis [Firth and Putnins, 2004]. However, HaCaT cells have anomalies that can modify their response to stress, including mutations in both alleles of the TP53 gene resulting in the absence of wild-type p53 protein in these cells [Lehman et al., 1993]. Thus, we checked the most interesting results of the microarray study in primary keratinocytes and confirmed the changes in energy metabolism in these normal cells.

The present results can be compared to those published in the literature. Many studies of the cell response to environmental stresses show that part of gene regulations aim at conserving energy. An immediate induction of ATP at 3 and 6 h after irradiation has been described in murine mammary carcinoma [Sijens et al., 1986]. In vivo studies have indicated a decrease of ATP at 24 h after a large range of doses, without addressing the response at early time points [Sijens et al., 1986, 1997; Orel et al., 2000]. Concerning keratinocyte energy metabolism, cell response of HaCaT to γ irradiation seems close to the response of primary keratinocytes to UVB, as induction of several mitochondrial proteins involved in the production of energy, such as ATP synthase, cytochrome-*c* oxidase and NADH dehydrogenase, and down-regulation of energy-requiring processes, such as lipid neogenesis, have also been described [Li et al., 2001]. Other regulations at 3 h, such as upregulation of the Na^+/K^+ pump, could reflect a mechanism for maintaining ionic gradients through membranes, which are important cellular targets for ionizing radiation.

In conclusion, we observed that irradiation induced a global and transient reprogramming at 3 h in human differentiated HaCaT keratinocytes. This early reprogramming resulted in an energy providing response, suggesting that the first wave of gene regulation seems to be essentially devoted to the maintenance of cell homeostasis. This immediate response was over at 24 h after exposure. For dosimetric applications, DNA array studies should be performed on longer time kinetics in order to search for markers of exposure both during the immediate and later waves of gene regulations. In irradiated keratinocytes, these later waves may be involved in the management of cell death and relationships with the cell microenvironment.

ACKNOWLEDGMENTS

The authors thank the Tissue Bank for Research (AFM-BTR, La Pitié-Salpétrière, Paris) for obtaining normal human skin biopsies, and Claude Sigalat (CEA, DBJC, Saclay) for helping in the ATP level measurements. We also acknowledge S. Cure, G. Lemaitre, and G. Munhoz-Essenfelder for critical reading of the manuscript.

REFERENCES

Ashburner M, Ball CA, Blake JA, Botstein D, Butler H, Cherry JM, Davis AP, Dolinski K, Dwight SS, Eppig JT, Harris MA, Hill DP, Issel-Tarver L, Kasarskis A, Lewis S, Matese JC, Richardson JE, Ringwald M, Rubin GM, Sherlock G. 2000. Gene ontology: Tool for the unification of biology. The Gene Ontology Consortium. Nat Genet 25:25–29.

Balcer-Kubiczek EK, Zhang XF, Han LH, Harrison GH, Davis CC, Zhou XJ, Ioffe V, McCready WA, Abraham JM, Meltzer SJ. 1998. BIGEL analysis of gene expression in HL60 cells exposed to X rays or 60 Hz magnetic fields. Radiat Res 150:663–672.

Birrell GW, Brown JA, Wu HI, Giaever G, Chu AM, Davis RW, Brown JM. 2002. Transcriptional response of *Saccharomyces cerevisiae* to DNA-damaging agents does not identify the genes that protect against these agents. Proc Natl Acad Sci USA 99:8778–8783.

Boukamp P, Petrussevska RT, Breitkreutz D, Hornung J, Markham A, Fusenig NE. 1988. Normal keratinization in a spontaneously immortalized aneuploid human keratinocyte cell line. J Cell Biol 106:761–771.

Breitkreutz D, Schoop VM, Mirancea N, Baur M, Stark HJ, Fusenig NE. 1998. Epidermal differentiation and basement membrane formation by HaCaT cells in surface transplants. Eur J Cell Biol 75:273–286.

Dazard JE, Gal H, Amariglio N, Rechavi G, Domany E, Givol D. 2003. Genome-wide comparison of human keratinocyte and squamous cell carcinoma responses to UVB irradiation: Implications for skin and epithelial cancer. Oncogene 22:2993–3006.

Firth JD, Putnins EE. 2004. Keratinocyte growth factor 1 inhibits wound edge epithelial cell apoptosis in vitro. J Invest Dermatol 122:222–231.

Fornace AJ, Jr., Alamo I, Jr., Hollander MC, Lamoreaux E. 1989. Induction of heat shock protein transcripts and B2 transcripts by various stresses in Chinese hamster cells. Exp Cell Res 182:61–74.

Hardmeier R, Hoeger H, Fang-Kircher S, Khoschsorur A, Lubec G. 1997. Transcription and activity of antioxidant enzymes after ionizing irradiation in radiation-resistant and radiation-sensitive mice. Proc Natl Acad Sci USA 94:7572–7576.

He YY, Huang JL, Sik RH, Liu J, Waalkes MP, Chignell CF. 2004. Expression profiling of human keratinocyte response to ultraviolet A: Implications in apoptosis. J Invest Dermatol 122:533–543.

Huang Z, Senoh Y, Katoh S, Miwa N. 2004. Preventive effects of a water-soluble derivative of chroman moiety of vitamin E on lipid hydroperoxide-induced cell injuries and DNA cleavages through repressions of oxidative stress in the cytoplasm of human keratinocytes. J Cell Biochem 92:425–435.

Lehman TA, Modali R, Boukamp P, Stanek J, Bennett WP, Welsh JA, Metcalf RA, Stampfer MR, Fusenig N, Rogan EM. 1993. p53 mutations in human immortalized epithelial cell lines. Carcinogenesis 14:833–839.

Lemaitre G, Lamartine J, Pitaval A, Vaigot P, Garin J, Bouet S, Petat C, Soularue P, Gidrol X, Martin MT, Waksman G. 2004. Expression profiling of genes and proteins in HaCaT keratinocytes: Proliferating versus differentiated state. J Cell Biochem 93:1048–1062.

Li D, Turi TG, Schuck A, Freedberg IM, Khitrov G, Blumenberg M. 2001. Rays and arrays: The transcriptional program in the response of human epidermal keratinocytes to UVB illumination. Faseb J 15:2533–2535.

Mendonca MS, Boukamp P, Stanbridge EJ, Redpath JL. 1991. The radiosensitivity of human keratinocytes: Influence of activated c-H-ras oncogene expression and tumorigenicity. Int J Radiat Biol 59:1195–1206.

Orel VE, Kadyuk IN, Dzyatkovskaya NN, Danko MI, Mel'nic YI. 2000. Mechanoluminescence: Lymphocyte analysis after exposure to ionizing radiation. Luminescence 15:29–36.

Sesto A, Navarro M, Burslem F, Jorcano JL. 2002. Analysis of the ultraviolet B response in primary human keratinocytes using oligonucleotide microarrays. Proc Natl Acad Sci USA 99:2965–2970.

Seymour CB, Mothersill C, Mooney R, Moriarty M, Tipton KF. 2003. Monoamine oxidase inhibitors l-deprenyl and clorgyline protect nonmalignant human cells from ionising radiation and chemotherapy toxicity. Br J Cancer 89:1979–1986.

Sijens PE, Bovee WM, Seijkens D, Los G, Rutgers DH. 1986. In vivo 31P-nuclear magnetic resonance study of the response of a murine mammary tumor to different doses of gamma-radiation. Cancer Res 46:1427–1432.

Sijens PE, Baldwin NJ, Ng TC. 1997. 31P magnetic resonance spectroscopy detection of response-predictive adenosine triphosphate decrease in irradiated radiation-induced fibrosarcoma-1 tumors. Invest Radiol 32:39–43.

Soares MB, Bonaldo MF, Jelene P, Su L, Lawton L, Efstratiadis A. 1994. Construction and characterization of a normalized cDNA library. Proc Natl Acad Sci USA 91:9228–9232.

Stokes MP, Michael WM. 2004. A novel replication arrest pathway in response to DNA damage. Cell Cycle 3:126–127.

Takao J, Ariizumi K, Dougherty II, Cruz PD, Jr. 2002. Genomic scale analysis of the human keratinocyte response to broad-band ultraviolet-B irradiation. Photodermatol Photoimmunol Photomed 18:5–13.

Tani H, Morris RJ, Kaur P. 2000. Enrichment for murine keratinocyte stem cells based on cell surface phenotype. Proc Natl Acad Sci USA 97:10960–10965.

Woloschak GE, Shearin-Jones P, Chang-Liu CM. 1990. Effects of ionizing radiation on expression of genes encoding cytoskeletal elements: Kinetics and dose effects. Mol Carcinog 3:374–378.